Research Square

Preprints are preliminary reports that have not undergone peer review.
They should not be considered conclusive, used to inform clinical practice,
or referenced by the media as validated information.

Characteristics of Fracture Distribution and Evaluation of Reservoir Effectiveness in the Chang 8 Formation of the Zhenjing Area, Ordos Basin

Guilin Yang

ygl829@yulinu.edu.cn

Yulin University

Yunyun Bai

Yulin University

Shuyue Ren

Yulin University

Article

Keywords: Fractures, Main controlling factors, Zhenjing area, Ordos Basin

Posted Date: November 1st, 2026

DOI: https://doi.org/10.21203/rs.3.rs-11302292/v1

License: This work is licensed under a Creative Commons Attribution 4.0 International License.
Read Full License

Additional Declarations: No competing interests reported.

Abstract

Objective

This study aims to clarify the developmental characteristics and effectiveness of natural fractures in the tight sandstone reservoir of the Chang 8 Formation within the Zhenjing area, Ordos Basin. Thereby providing a geological basis for favorable zone evaluation and development planning.

Methods

Integrating core observations, field outcrop surveys, image logs, and three-dimensional seismic data, we employ maximum-likelihood fracture detection, statistical analyses of strike and dip, density calculations, and filling-degree evaluations to systematically investigate fracture genesis, geometric distribution, and controlling factors. A comprehensive framework for fracture effectiveness assessment is subsequently established.

Results

Fractures in the study area are predominantly tectonic. Geometrically, high-angle oblique and vertical fractures are dominant, with strikes mainly oriented NEE and NWW, reflecting the overprint of multiple tectonic episodes. The average density of fractures is 1.04 per meter. The overall development is relatively high, but it is relatively poor in the southeast area. The lengths are mostly concentrated between 10 and 20 centimeters, and the extensibility is good. Fracture distribution is jointly controlled by fault activity, lithological variations, and the thickness of rock layers, resulting in a heterogeneous pattern of " faults governing the plane distribution, lithology controlling the strata, and thickness dictating the density ". Effectiveness evaluation reveals that fractures in sandstone (63.87%) are significantly more effective than those in mudstone (43.83%). The smaller the angle between the fracture orientation and the current maximum principal stress direction, the larger the fracture opening, and the lower the filling degree, the higher the effectiveness. Increased burial depth generally reduces fracture aperture, although near-vertical fractures are less affected. Cementation adversely affects effectiveness, whereas dissolution and micro-fracturing can enhance connectivity.

Conclusion

Fracture effectiveness results from the synergistic interplay of tectonic stress, burial depth, and diagenetic evolution. The findings offer a geological foundation for fractured-reservoir evaluation and well-site deployment in the Chang 8 interval of the Zhenjing area.

1 Introduction

The Ordos Basin, located in the western part of the North China Craton, is bounded by several primary structural units, including the Jinxi Fault Belt to the east, the Western Margin Thrust Belt and Tianhuan Depression to the west, the Weibei Uplift to the south, and the Yimeng Uplift to the north [1–6]. The basin has undergone three phases of tectonic activity. During the Indosinian period, NWW-trending strike-slip faults were generated under north-south compressive stress, accompanied by nearly east-west parallel faults. During the Yan Shan period, NNE-trending faults formed under NW–SE left-lateral shear compression. During the Himalayan period, smaller-scale NEE-trending faults developed under NW–SE extensional and NE compressional stresses, while pre-existing faults were reactivated [6–8]. As a result of multiple tectonic movements, the transitional zone along the basin margin now hosts a dense network of faults and fractures, which provide excellent channels and spaces for the migration and accumulation of oil and gas.

The Zhenjing area is situated at the junction of the Tianhuan Syncline, the Northern Shaanxi Slope, the Weibei Uplift, and the western margin thrust belt, thus occupying a unique tectonic position [7, 9–11]. Its primary production layer is the Chang 8 oil formation, with an average porosity of 10.7% and a permeability of 0.4 mD, which is a typical low-porosity and low-permeability reservoir [10]. As exploration and development have advanced, it has been discovered that the main high-yield areas are not composed of high-quality sand bodies, which has become a significant contradiction between the deployment of conventional well locations and actual production. Consequently, increasing attention has been directed toward the role of fractures, and extensive structural analyses have been conducted. However, no comprehensive evaluation of fracture characterization accuracy and effectiveness has yet been performed, hampering further development. Therefore, clarifying the characteristics of fracture development in tight reservoirs, establishing a quantitative evaluation system for fracture effectiveness, and deeply analyzing the main controlling factors and temporal-spatial evolution patterns of fractures are the key scientific prerequisites for accurately conducting the evaluation of favorable zones.

2 Characteristics and Distribution Patterns of Fractures

Using core observations, field outcrop data, image logs, and drilling information, we analyzed the fracture characteristics of the Chang 8 formation in the Zhenjing area, including fracture genesis, orientation, dip angle, density, and controlling factors.

2.1 Fracture Genesis and Types

To clarify the genetic types of fractures, this paper adopted the classification scheme proposed by Zhou Wen (1998) [12]. Based on core observations from 112 cored wells and field profile surveys around the study area, fractures in the Chang 8 reservoir can be divided into two categories: diagenetic fractures formed during burial diagenesis and tectonic fractures generated under structural stress (Fig. 1). Tectonic fractures are the dominant type and, by mechanical genesis, can be further subdivided into shear and tensile fractures. Tensile fractures are characterized by short, irregular traces and rough surfaces, typically filled with calcite, and formed under a tensile stress regime (Fig. 1a). In contrast,

shear fractures exhibit long, straight, and regular surfaces, commonly with minor offsets and kinematic indicators such as stepped features, indicating a shear-stress environment (Fig. 1b).

Based on their geometric relationship with the bedding planes, tectonic fractures are classified as joint-type or fault-type [13–14]. Joint-type fractures are vertically restricted to individual beds, with fracture heights approximately equal to bed thickness. The mechanical properties of the rock at the end of the fracture are relatively weak(Fig. 1a). Fault-type fractures are larger and cross-cut bedding planes (Fig. 1b, d). They often result from high-magnitude tectonic stress but may also develop by vertical propagation from joint-type fractures, terminating at brittle-plastic interfaces; such fractures have steep dips and long extension length.

Diagenetic fractures developed along micro-laminae, formed during diagenesis through compaction and dissolution. Core observations show that they are typically curved, discontinuous, branched, tapered, or merged along bedding planes, and are mainly controlled by sedimentary facies and diagenetic processes. In the study area, diagenetic fractures are primarily horizontal bedding fractures (Fig. 1c) and diagenetic contraction fractures (Fig. 1e).

Microfractures are commonly developed in fine-grained sandstones, siltstones, and mudstones, appearing as cutting patterns through mineral grains—an indication of intense mechanical deformation (Fig. 1f, g, h). They are classified into three types: intergranular, grain-edge, and intragranular fractures[15]. Intergranular fractures cut across multiple grains and are the predominant type in the study area, characterized by long traces and relatively large scale (Fig. 1f); some are filled with quartz or calcite. Grain-edge (intergranular) fractures develop along the margins of quartz or feldspar grains (Fig. 1g). Intragranular fractures occur within individual mineral grains or rock fragments at point-line contacts (Fig. 1h); they generally do not penetrate entire grains, have complex and variable orientations, and are mostly sub-perpendicular to grain contact surfaces. Both intragranular and grain-edge fractures are relatively small in scale and width, primarily influenced by mechanical compaction and hydrolytic dissolution, and are thus classified as diagenetic. These microfractures serve as important conduits connecting matrix pores and intragranular dissolution vugs [13–14, 16]. They can enhance subsurface fluid flow and improve reservoir quality, providing a foundation for macrofracture development and contributing to increased porosity and permeability.

2.2 Characteristics of Fracture Distribution

Before the characteristics of fracture analysis, we performed preliminary fracture detection using the maximum-likelihood method on 3D seismic data. The results showed that the fractures were densely developed (Fig. 2) [4]. Rose diagrams of fracture orientations derived from core and image-log data indicate that the Yanchang Formation in the Zhenjing area contains a diverse fracture system, including NEE, NWW, NE, NW, near-EW, and near-SN trends, with NEE- and NWW-oriented fractures being dominant (Fig. 2)—a consequence of multiple tectonic movements. Orientation measurements from image logs and cores show that high-angle oblique to vertical fractures account for over 65% of all fractures in both datasets. The fracture density is the highest, ranging from 0.7 to 1.65 fractures per meter. Whereas

low-angle oblique and horizontal fractures constitute a smaller proportion and have the lowest densities, both below 0.2 fractures per meter (Fig. 3a). Thus, the Yanchang Formation in the study area is characterized by the predominant development of high-angle fractures, with low-angle and horizontal fractures being relatively sparse.

Fracture development intensity can be described and evaluated using fracture density. Statistical analysis of core and image-log data indicates that fractures with densities of 0~2 fractures per meter account for over 70% of the total, and a small number of fracture sections density exceeding 3 fractures per meter (Fig. 3b). The development degree of the fractures varies significantly in different parts of the area (Figure 2)[4]. Core- observed fracture densities range from 0.06 to 4.6 fractures per meter, averaging 1.24 fractures per meter; image-logging-interpreted densities range from 0.21 to 3.09 fractures per meter, averaging 0.84 fractures per meter. Overall, the study area shows a high degree of fracture development with local variations; the southeastern part exhibits relatively lower fracture intensity compared to other regions (Fig. 2). The extent of the fracture is governed by rock mechanical properties, and fracture lengths typically range from 10 to 20 cm, with the longest recorded at 265 cm, indicating good extensibility.

2.3 Controlling Factors of Fracture Distribution

As described above, multiple sets of fractures have developed in the study area due to multiple tectonism. Statistical analysis of the relationship between fracture density and distance from major faults reveals a strong correlation: the closer to a major fault, the higher the fracture density (Fig. 4a). This is primarily because fault activity induces localized stress perturbations, creating zones of stress concentration and enhanced fracturing in the vicinity. Consequently, faults are a key control on fracture development and distribution [13, 16].

Lithology also exerts a significant influence on the development of fractures, as shown by core statistics. The highest fracture densities are observed in siltstone, silty mudstone, and fine sandstone, whereas silty mudstone and mudstone display lower intensities (Fig. 4b). Consequently, sandstone intervals exhibit far greater fracture development than mudstone intervals. The lithological factors causing this difference primarily include grain size, mineral composition, and porosity. Grain size and porosity reflect compaction degree, which in turn affects brittleness: finer grains and lower porosity lead to more compact rocks that are more prone to fracturing [17–20]. Mineral composition affects mechanical strength. Among the clastic components, quartz and feldspar are the dominant minerals, with quartz averaging 29% and feldspar 26% [10]. Both are brittle minerals, and higher contents generally promote fracturing. In the study area, brittle minerals are mainly concentrated in sandstones and are nearly absent in mudstones, which is a primary reason for the differential fracture distribution.

Based on statistical analysis of fractured bed thickness versus fracture density from core data, we constructed a cross-plot for the Chang 8 formation (Fig. 4c). The figure shows a relatively strong positive correlation between bed thickness and fracture density: as bed thickness increases, fracture density decreases, and when bed thickness exceeds 2 m, the density declines rapidly (Fig. 4c). This is because

thicker beds have greater resistance to structural failure, making them less susceptible to fracturing [13, 18].

3 Evaluation of Fracture Effectiveness

The Chang 8 reservoir in the study area is characterized by low porosity and low permeability, with poor storage and flow capacity. Fractures can significantly enhance permeability and provide effective storage space, which is the primary focus of fracture effectiveness assessment [13]. The degree of fracture infilling, the extent of fracture extension and aperture, and the connectivity collectively govern fluid flow capacity and storage performance, thereby determining whether a fracture is effective [13, 18, 21–22].

3.1 Evaluation of Fracture Effectiveness

Based on the degree of infilling, fractures are classified as completely filled, partially filled, or unfilled. Partially filled and unfilled fractures can provide effective migration pathways and storage space for hydrocarbons and are therefore considered effective. Completely filled fractures offer virtually no contribution to migration or storage and are deemed ineffective [4, 16]. The higher the degree of infilling, the poorer the connectivity and effectiveness; conversely, lower infilling corresponds to better connectivity and effectiveness. Fracture fills in the study area consist mainly of calcite, with minor carbonaceous and muddy, etc. Statistical analysis of filling conditions for different lithologies reveals that in mudstones, completely filled fractures account for 56.17%, while partially filled and unfilled fractures account for 22.83% and 21.00%, respectively—i.e., effective fractures constitute 43.83% and ineffective fractures 56.17%. In sandstones, completely filled fractures account for 36.13%, while partially filled and unfilled fractures account for 32.17% and 31.70%, respectively—effective fractures thus comprise 63.87% and ineffective 36.13% (Fig. 5a). These data indicate that fracture effectiveness in mudstones is lower than in sandstones (Fig. 5a).

Fracture aperture not only describes the intensity of the fracture size but also serves as an important parameter for effectiveness assessment [16, 18]. Through interpretation of apertures from image logs and direct core measurements, followed by statistical analysis, we find that apertures below 1 mm account for approximately 81% of the total. Apertures in the ranges of 3.5~4 mm and 1.5~2 mm account for 7.6% and 5.1%, respectively. The maximum recorded aperture is 5.8 mm (Fig. 5b). Apertures greater than 1 mm are predominantly observed in sandstones, whereas mudstones show lower opening degrees, mainly due to their higher plasticity.

3.2 Factors Governing Fracture Effectiveness

(1) The current tectonic stress field

The current tectonic stress field is a key factor influencing fracture effectiveness. When the current maximum principal stress is nearly parallel to fracture strike, the fracture plane experiences relative tension, increasing aperture and enhancing effectiveness. Conversely, when the stress direction is nearly

perpendicular to fracture strike, aperture is small, connectivity is poor, and effectiveness is low[4,13]. It is generally accepted that the direction of the current maximum principal stress aligns with that of drilling-induced tensile fractures. Based on previous studies on fracture evolution in the Zhenjing area [23–25], the maximum principal stress direction is generally NEE, at an angle of approximately 55.12° [4–6]. Correlation analysis between fracture strike and the angle to the current maximum principal stress shows a negative correlation: the smaller the angle, the larger the aperture, the lower the degree of infilling, and the higher the effectiveness—core observations also indicate higher oil shows (Fig. 6a). Conversely, a larger angle results in greater normal stress acting on the fracture plane, reduced aperture, decreased effectiveness. This is because fractures more parallel to the current stress field are more conducive to satisfying slip conditions under the regional stress regime. Overall, fractures with smaller angles between strike and current stress direction exhibit significantly higher effectiveness than those with larger angles.

(2) Burial depth

Burial depth is also an important factor controlling fracture effectiveness [18]. Analysis of the relationship between burial depth and fracture aperture in the Chang 8 formation reveals that, overall, aperture decreases with increasing depth (Fig. 6b). The primary reason is that at greater depths, higher overburden pressure acting on fracture surfaces reduces aperture and thus effectiveness. However, some fractures in the study area are near-vertical; in such cases, the overburden pressure acts nearly perpendicular to the fracture plane, and aperture is virtually unaffected by burial depth.

(3) Diagenesis

Cementation fills and occludes fractures, reducing effectiveness and impairing reservoir physical properties [25–26]. Siliceous cementation is widely developed in the Chang 8 reservoir, mainly as quartz overgrowths (Fig. 7a), while carbonate cementation is dominated by calcite (Fig. 7b). The prolonged cementation history of the target formation, together with high fracture infilling and low effectiveness, is a primary cause of reservoir compaction. Following tectonic uplift and hydrocarbon migration, feldspar and rock fragments in the Chang 8 formation underwent dissolution and erosion by organic acids (Fig. 7c). This dissolution can reopen previously filled fracture spaces, thereby enhancing effectiveness, mainly during late diagenesis and mid-diagenetic stage A [10]. Additionally, microfractures generated by fracturing can effectively connect pores (Fig. 7d), which is crucial for improving reservoir properties.

4 Conclusions

(1) Fractures in the Chang 8 reservoir of the Zhenjing area are predominantly tectonic in origin. Geometrically, they are mainly high-angle oblique to vertical fractures, with dominant strikes in the NEE and NWW directions, reflecting the overprint of multiple tectonic events. The average fracture density is 1.04 fractures per meter; development is generally intense, though relatively weaker in the southeast. Fracture lengths are mainly concentrated in the 10–20 cm range, with the longest reaching 265 cm, indicating good extensibility.

(2) The distribution and intensity of fractures are jointly controlled by fault activity, lithological variations, and bed thickness. Fault activity creates peripheral stress-concentration zones, and fracture density increases with proximity to faults. Sandstones, with higher contents of brittle minerals such as quartz and feldspar, exhibit significantly greater fracture development than mudstones. Fracture density decreases with increasing bed thickness, and thin layers (< 2 m) are more prone to fracturing. The interactions among these factors vary in mode and intensity, collectively forming a heterogeneous fracture distribution pattern characterized by “faults governing the plane distribution, lithology controlling the strata, and thickness dictating the density.”

(3) Fracture effectiveness is primarily determined by the degree of infilling and aperture. In the study area, sandstone fractures are markedly more effective than those in mudstones, constituting the primary effective reservoir and permeable space. The smaller the angle between fracture strike and the current maximum principal stress, the larger the aperture, the lower the infilling degree, and the higher the effectiveness. With increasing burial depth and overburden pressure, aperture generally decreases and effectiveness declines; however, near-vertical fractures are less affected by depth. Cementation significantly reduces effectiveness, whereas dissolution and microfracturing can improve connectivity and enhance reservoir properties. The synergistic interplay of these three factors indicates that fracture effectiveness is not determined by a single factor, but rather by the combined effects of tectonic stress, burial depth, and diagenetic evolution.

Declarations

Author Contribution

Yang. wrote the main manuscript text. Ren and Bai. prepared figures 3-4. All authors reviewed the manuscript.

Acknowledgements

This study was jointly funded by the Shaanxi Provincial Department of Education Special Project (No. 23JK0758), Project of Shaanxi Provincial Science and Technology Department (No. 2026JC-YBQN-035), the Yulin Municipal Science and Technology Bureau Industry-Academia-Research Collaboration Project (No. 2023CXY129), the Yulin Municipal Young Talent Support Programme (No. 20230511), and the Yulin University High-Level Talent Research Start-up Fund (No. 2023GK61).

Data Availability

The datasets used and/or analysed during the current study available from the corresponding author on reasonable request.

References

1. Ren Zhanli, Zhang Sheng, Gao Shengli, et al. Discussion on the Abnormal Distribution Area and Formation Period of Thermal Evolution Degree in the Ordos Basin [J], Acta Geologica Sinica, 2006, 80(5): 674-682.
2. Dai Jinxing, Ni Yunyan, Yang Zhi, Hu Guoyi, Gong Deru, Huang Shipeng... & Liao Fengrong. (2026). The Ordos Super Gas Basin. World Petroleum Industry, 33(Z1), 1-20.
3. Ren Zhanli, Research on the Tectonic Thermal Evolution History of Sedimentary Basins in Northern China [M]. Petroleum Industry Press. 1996.
4. Guilin Yang, Zhanli Ren, Yuanyuan Zhang, Kai Qi; Prediction and research of fracture distribution characteristics of the Chang 8 reservoir in Zhenjing area, Ordos Basin. Interpretation 2022; 10 (4): B25–B35.
5. Ren Zhanli, Qi Kai, Liu Runchuan, Cui Junping, Chen Zhipeng, Zhang Yuanyuan, Yang Guilin, Ma Qian. The formation dynamic background of the Early Cretaceous tectonic thermal event in the Ordos Basin and its control on the formation (mining) period of various minerals such as oil and gas [J]. Chinese Journal of Geology, 2020, 36(04): 1213-1234.
6. Yang Guilin, Ren Zhanli, He Faqi, et al. The development characteristics of fault bodies and the oil and gas enrichment rules in the Zhenjing area on the southwest margin of the Ordos Basin [J]. Oil and Gas Geology, 2022, 43(6): 1382-1396.
7. Wang Baojiang, Wu Zhenfeng, Ji Waiying, et al. Fault body fracture identification and interpretation at high-angle slip - a case study of the Zhenjing block in the Ordos Basin [J]. Natural Gas Geoscience, 2025, 36(1): 142-154.
8. Zhang Yuanyuan, Ren Zhanli, He Faqi, Cui Junping, Yang Guilin, Wang Kun, Ji Yuanyuan. The tectonic characteristics of the Mesozoic-Cenozoic in the structural turning area of the craton basin and its control significance - Taking the Yanchang Formation in the Zhenjing area in the southwest of the Ordos Basin as an example [J]. Chinese Journal of Geology, 2020, 36(11): 3537-3549.
9. He Faqi, Liang Chengchun, Lu Cheng, Yuan Chunyan, Li Xiaowei. Identification and description of fault bodies in the tight-low-permeability oil reservoirs in the transitional zone of the southern margin of the Ordos Basin [J]. Oil and Gas Geology, 2020, 41(04): 710-718.
10. Yang, G.; Ren, Z.; Qi, K. Research on Diagenetic Evolution and Hydrocarbon Accumulation Periods of Chang 8 Reservoir in Zhenjing Area of Ordos Basin. Energies 2022, 15, 3846.
11. Zhang Yuanyuan, Ren Zhanli, He Faqi, et al. Structural Transition Zone of the Kaltong Basin - Structural Characteristics of Mesozoic-Cenozoic Strata and Their Hydrocarbon Reservoir Control Significance: A Case Study of the Yinzhen Area in the Southwest of the Ordos Basin [J]. Chinese Journal of Geology, 2020, 36(11): 3537-3549.
12. Zhou Wen. Evaluation Methods for Fractured Oil and Gas Reservoirs [M]. Chengdu: Sichuan Science and Technology Press, 1998.

13. Suo Xiaocen, Gong Lei, Fu Xiaofei, et al. Fracture Distribution Characteristics and Effectiveness Evaluation of the 7th Member of the Yancheng Formation in the Sanbian Area of the Ordos Basin [J]. Earth Science, 2023, 48(7): 2601-2613.
14. Zeng Lianbo, Lu Peng, Qu Xuefeng, Fan Jianming. Multi-scale Fractures in Compact Low Permeability Reservoirs and Their Geological Conditions of Formation [J]. Oil and Gas Geology, 2020, 41(03): 449-454.
15. Lv Wenya, Zeng Lianbo, Zhou Siben, et al. Microscopic Fracture Characteristics and Control Factors of Compact Sandstone Reservoirs in the Southwest of the Ordos Basin - Taking the Chang8 Reservoir of Honghe Oilfield as an Example [J]. Natural Gas Geoscience, 2020, 31(01): 37-46.
16. Wang Cuili. Research on Fracture Development Characteristics and Distribution Evaluation of the Chang9 Oil Layer Group in the Zhenjing Exploration Area [D]. Chengdu University of Technology, 2012.
17. Luo Yanling. Natural Fracture Characteristics of the Chang8 Reservoir in Honghe Oilfield of the Ordos Basin and Their Impact on Development [J]. Oil Geology & Engineering, 2020, 34(03): 52-56.
18. Liu Yan. Characteristics of Fractures in Low Permeability Reservoirs and Their Control Effect on Hydrocarbon Accumulation [D]. Chengdu University of Technology, 2013.
19. Gong Lei, Zeng Lianbo, Pei Senqi, Zhang Benjian, Gao Zhiyong, Zu Kewei, Li Honglin. Fracture Characteristics and Genesis of the Compact Sandstone Reservoir in the Qiansheng Section of the Xingsheng Formation [J]. Geological Science, 2013, 48(01): 217-226.
20. Wang Meng. Development Characteristics of Mesozoic Faults in the Zhenyuan-Jingchuan Area of the Ordos Basin [J]. Faulted Oil and Gas Fields, 2019, 26(02): 142-146.
21. Jiang Longyan. Fracture Characteristics of the Chang8 Member and Its Logging Identification in the Zhenjing Area [J]. Journal of Engineering Geophysics, 2017, 14(04): 475-480.
22. Liu Geyun, Huang Chenjun, Zhou Xingui, et al. Quantitative Evaluation of Fracture Development Degree of the Triassic Yancheng Formation in the Ordos Basin [J]. Petroleum Exploration and Development, 2015, 42(4): 444-453.
23. Zhou Xinggui, Zhang Linyan, Huang Chenjun, et al., 2012. Fracture Distribution Model and Fracture Effectiveness of the Long6-3 Reservoirs. Journal of Jilin University (Earth Science Edition), 42(3): 689-697.
24. Wang Ke, Yang Haijun, Zhang Huiliang, et al., 2018. Structural Fracture Characteristics and Effectiveness of Ultra-Deep Compact Sandstone Reservoirs - Taking the Keshen8 Gas Reservoir in the Kuqa Depression of the Tarim Basin as an Example. Oil and Gas Geology, 39(4): 719-729.
25. Mao Zhe, Zeng Lianbo, Liu Guoping, et al., 2020. Fractures and Their Effectiveness of the Jurassic Deep Compact Sandstone Reservoirs in the Southern Margin of the Junggar Basin. Oil and Gas Geology, 41(6): 1212-1221.
26. Guo Xuanhao, Tan Chengqian, Zhao Junhui, et al., 2021. Differences in the Effects of Diagenesis on the Microstructure of Compact Sandstone Reservoirs - Taking the Chang7 Member in the

Zhongyuan and Zhenbei Areas of the Ordos Basin as an Example. Natural Gas Geoscience, 32(6): 826-835.

Figures

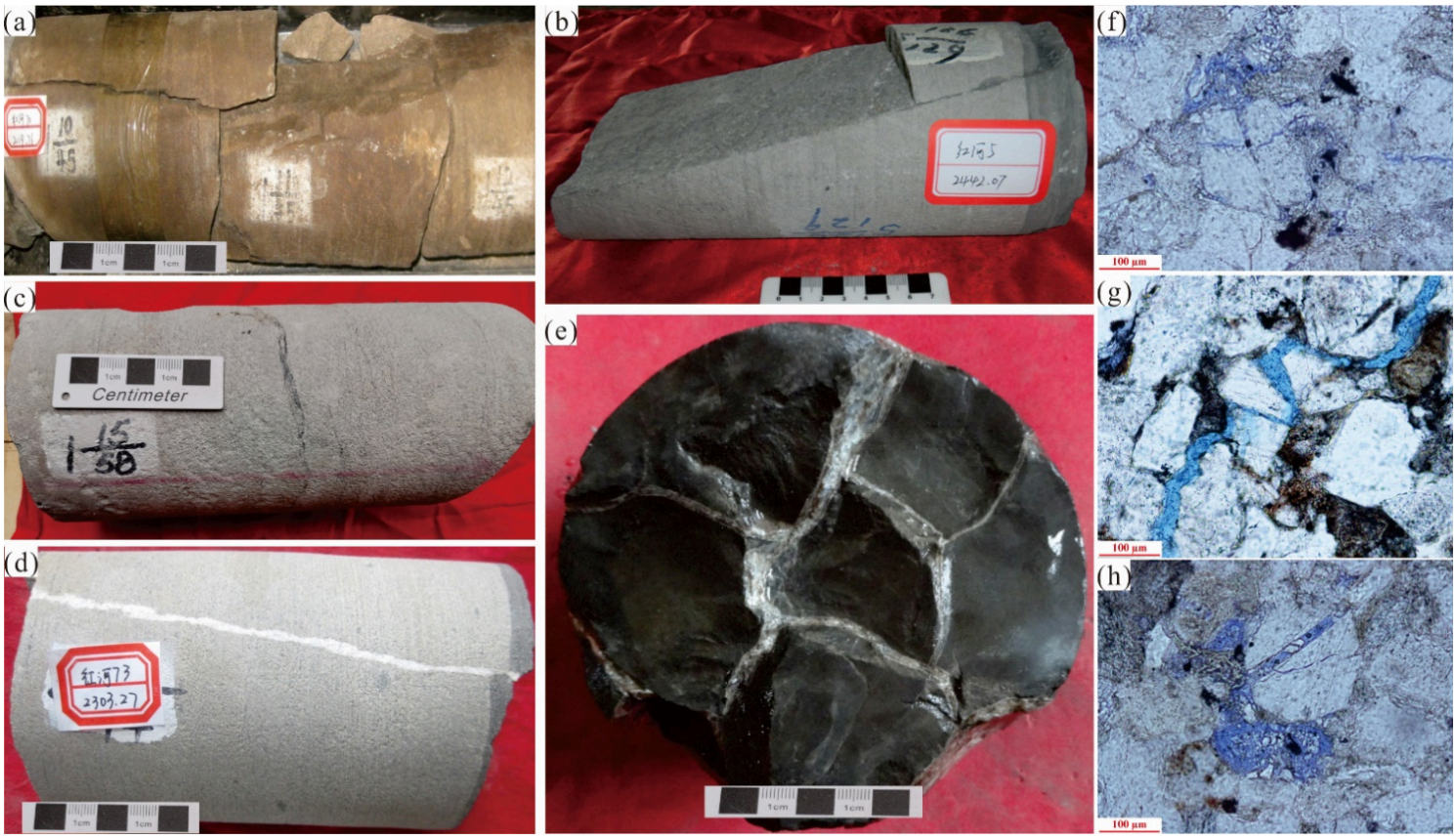


Figure 1

Core - Microscopic Fracture Photograph

(a) Tensile fracture, Well HH70, 2119.8 m; (b) Shear fracture, Well HH5, 2442 m; (c) Bedding fracture, Well HH183, 2165.75 m; (d) Fault-type fracture, Well HH73, 2303.27 m; (e) Contraction fracture, Well ZT4, 2049.9 m; (f) Intergranular fracture, Well ZT3, 2068.83 m; (g) Grain-edge fracture, Well ZJ19, 2296.585 m; (h) Intragranular fracture, Well ZT3, 2060.89 m

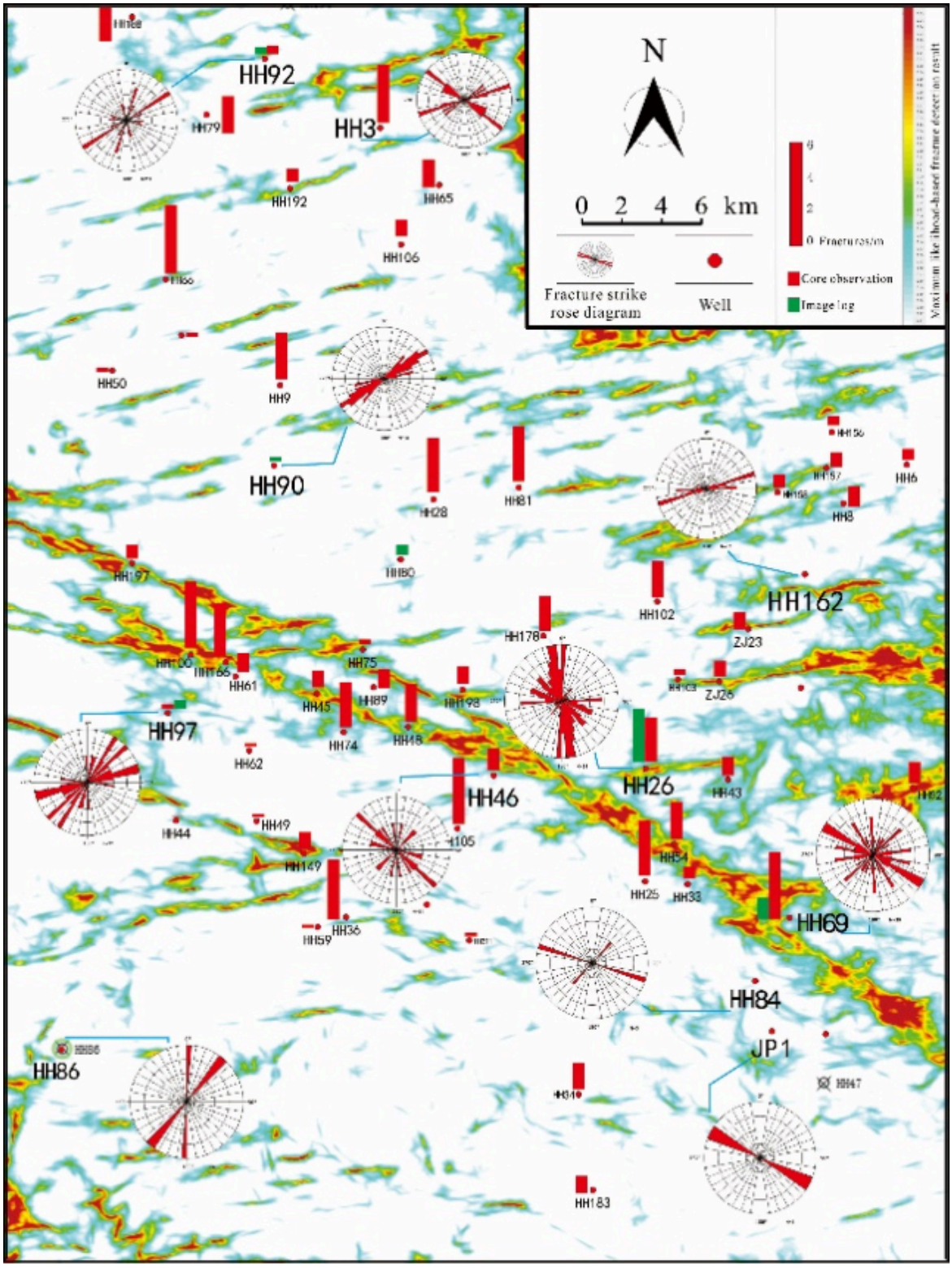


Figure 2

Comprehensive analysis of fracture characteristics

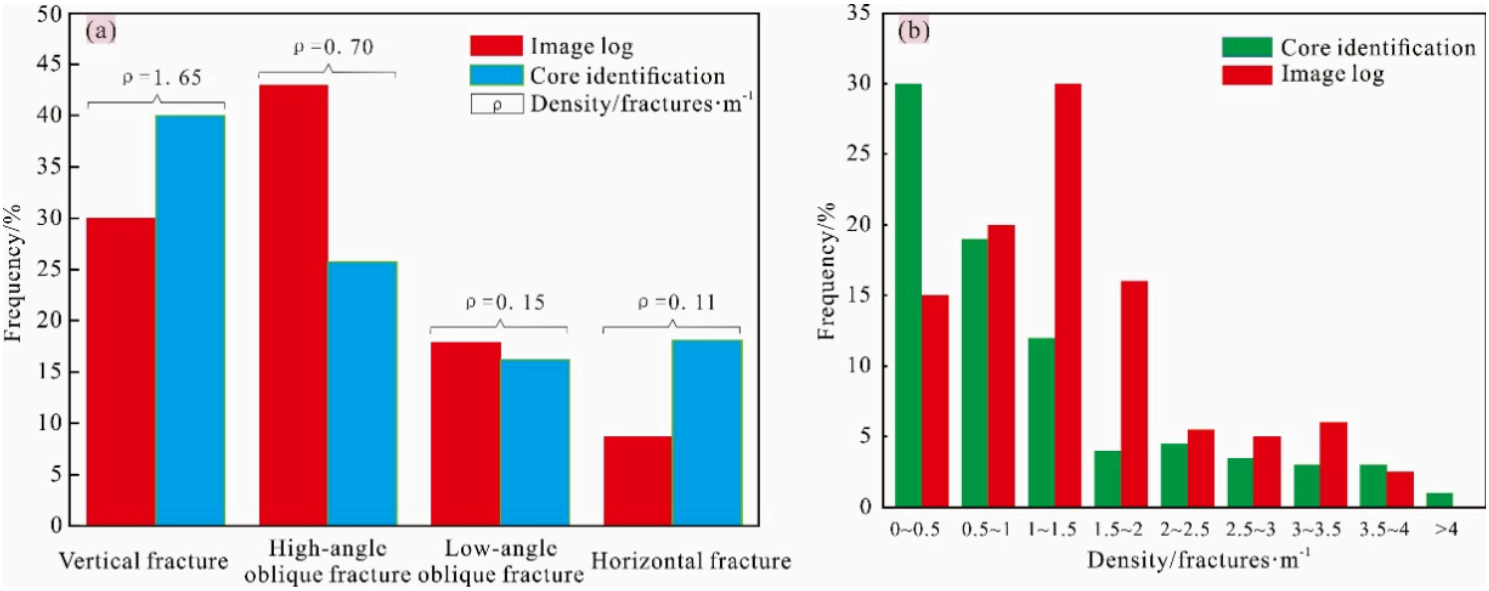


Figure 3

Histograms of fracture orientation–density distribution

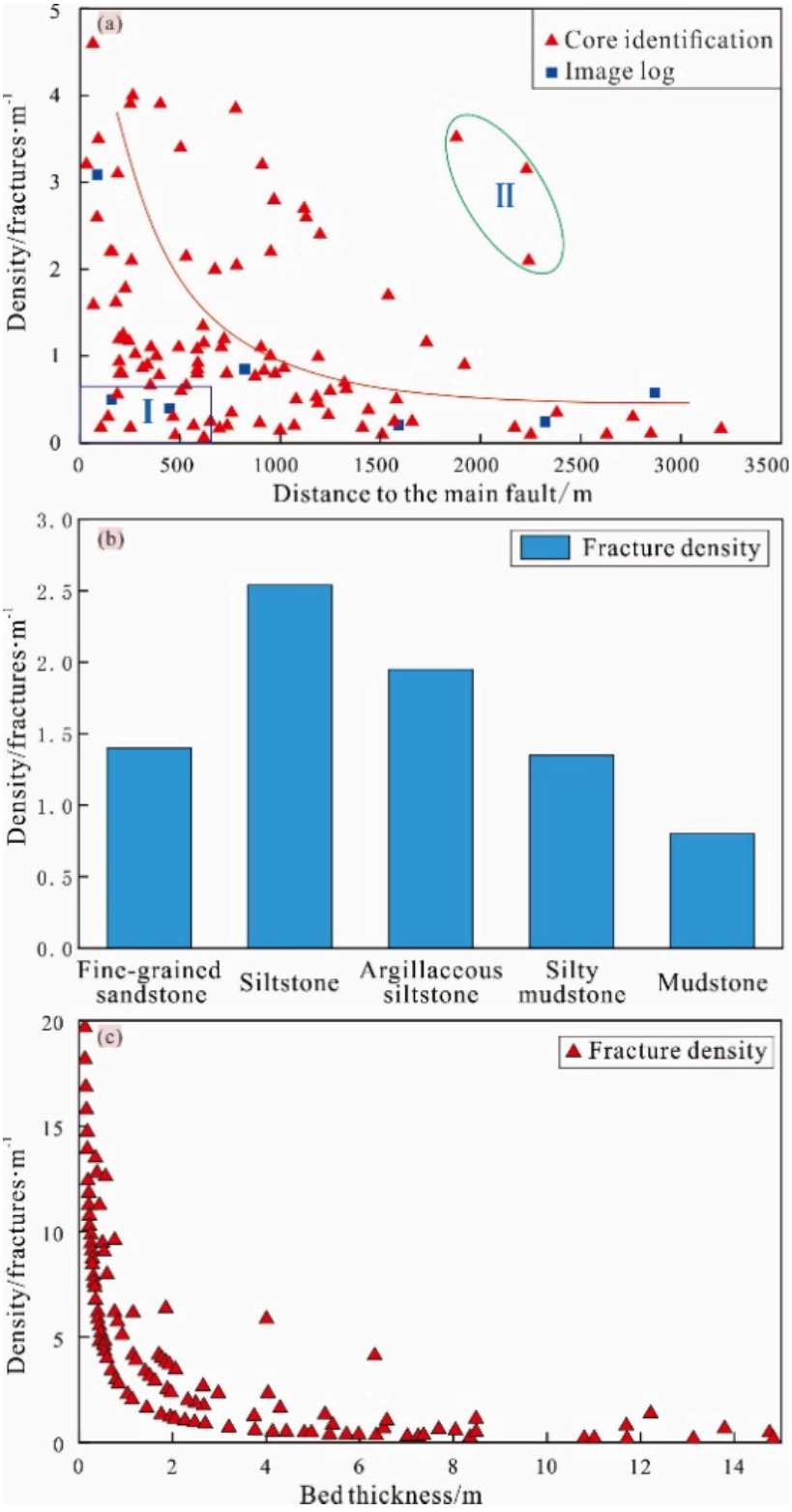


Figure 4

Comprehensive analysis of the main controlling factors of fracture distribution

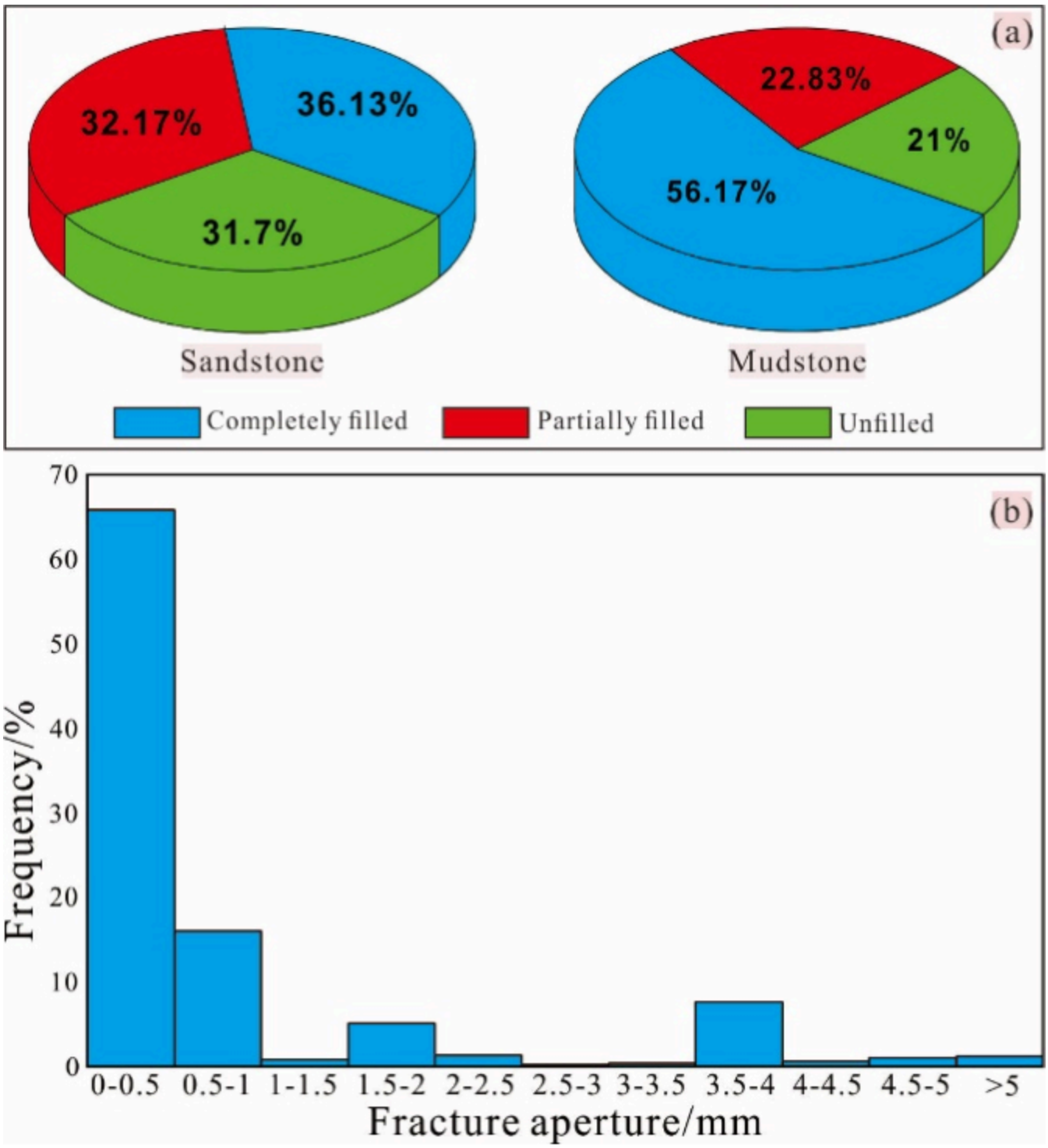


Figure 5

(a) Pie chart of fracture filling degree; (b) Histogram of fracture aperture frequency distribution

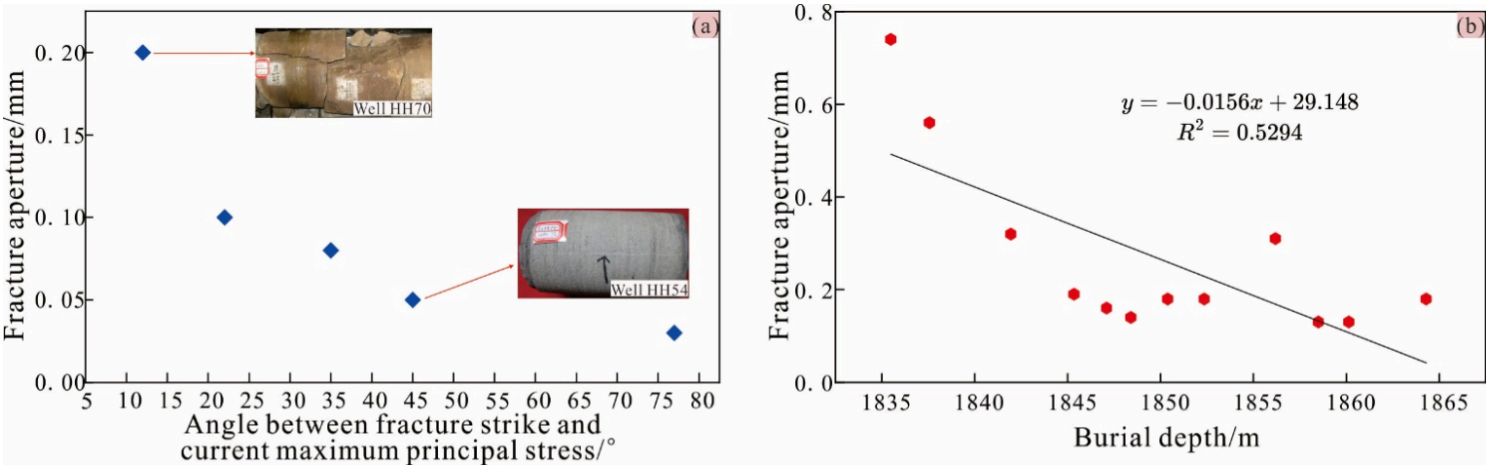


Figure 6

Cross plots of (a) fracture aperture vs. angle between fracture strike and current maximum principal stress, and (b) fracture aperture vs. burial depth.

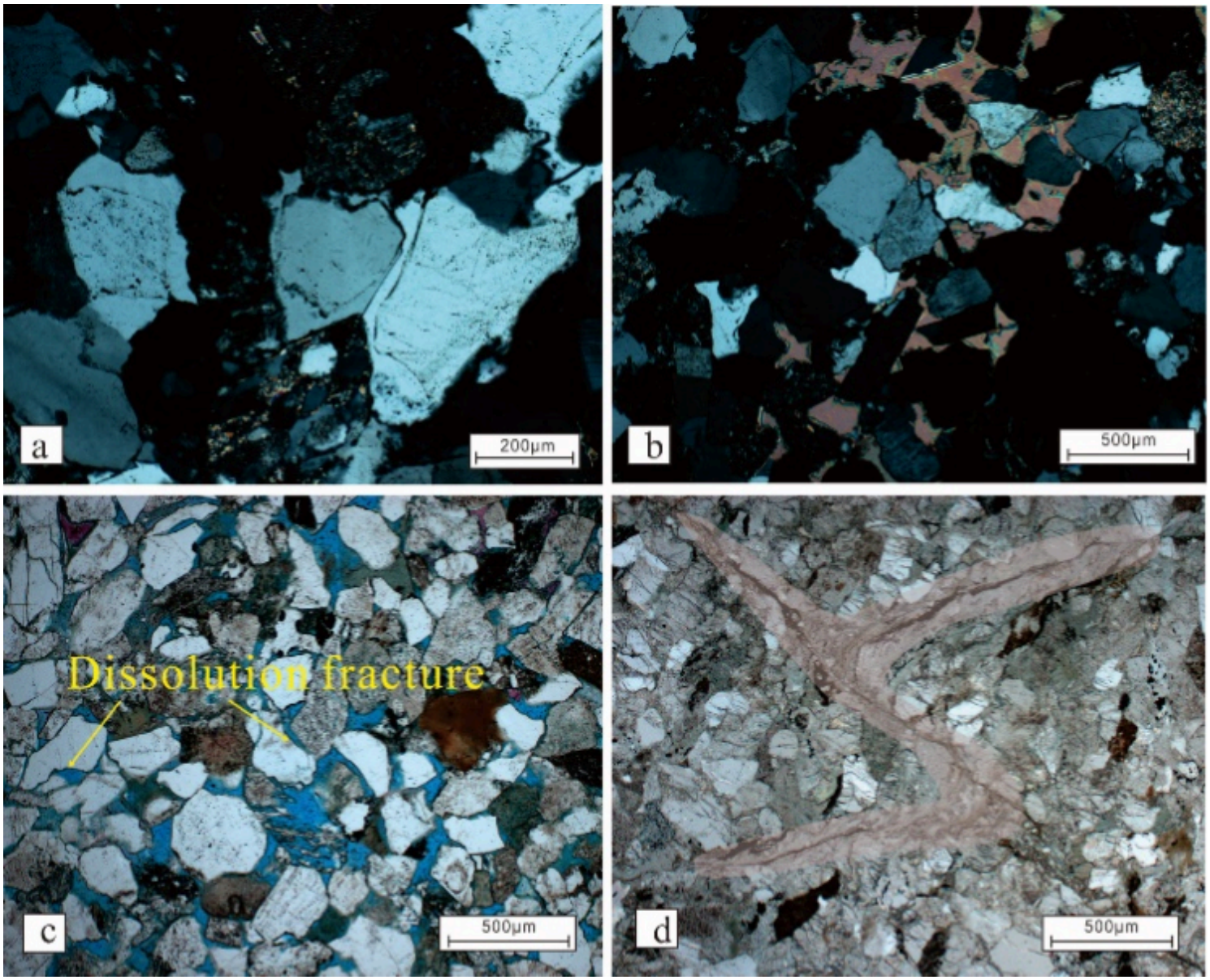


Figure 7

Microscopic characteristics of different diagenetic processes in the Chang 8 reservoir, Zhenjing area

(a) Quartz overgrowth, Well HH193, 2298.85 m, cross-polarized light, 100×; (b) Porous calcite cementation, Well HH193, 2299.7 m, cross-polarized light, 50×; (c) Dissolution vugs from feldspar dissolution, Well HH193, 2295.08 m, plane-polarized light, 50×; (d) Intersecting microfractures, Well HH166, 2396.87 m, plane-polarized light, 50×